AD-A093 749 DEFENSE MAPPING AGENCY HYDROGRAPHIC/ TOPOGRAPHIC CENT--ETC F/G 17/7
PRODUCTION OF LORAN-C RELIABILITY DIAGRAMS AT THE DEFENSE MAPPI--ETC(U)
NOV 80 C L WORRELL

UNCLASSIFIED NL

END
DATE FILMED
2-81
DTIC

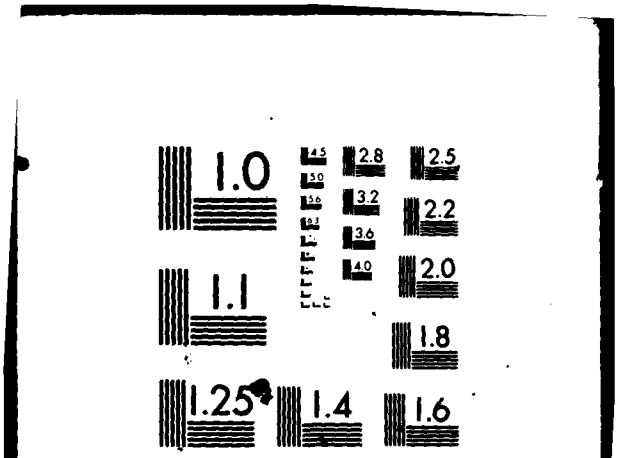

UNCLASSIFIED

LEVEL II

SECURITY CLASSIFICATION OF THIS PAGE *(When Data Entered)*

REPORT DOCUMENTATION PAGE		READ INSTRUCTIONS BEFORE COMPLETING FORM
1. REPORT NUMBER Institute of Navigation National Marine Meeting, New Orleans	2. GOVT ACCESSION NO. AD-A093749	3. RECIPIENT'S CATALOG NUMBER
4. TITLE *(and Subtitle)* Production of LORAN-C Reliability Diagrams at the Defense Mapping Agency		5. TYPE OF REPORT & PERIOD COVERED N/A
		6. PERFORMING ORG. REPORT NUMBER N/A
7. AUTHOR(s) CLARENCE L. WORRELL		8. CONTRACT OR GRANT NUMBER(s) N/A
9. PERFORMING ORGANIZATION NAME AND ADDRESS DMA Hydrographic/Topographic Center Washington, D.C. 20315		10. PROGRAM ELEMENT, PROJECT, TASK AREA & WORK UNIT NUMBERS N/A
11. CONTROLLING OFFICE NAME AND ADDRESS DMAHTC ATTN: PPTD (Tech. Pubs.) Washington, D.C. 20315		12. REPORT DATE 18-20 November 1980 13. NUMBER OF PAGES 9
14. MONITORING AGENCY NAME & ADDRESS*(if different from Controlling Office)*		15. SECURITY CLASS. *(of this report)* UNCLASSIFIED 15a. DECLASSIFICATION/DOWNGRADING SCHEDULE

16. DISTRIBUTION STATEMENT *(of this Report)*

Approved for public release; distrubution unlimited.

17. DISTRIBUTION STATEMENT *(of the abstract entered in Block 20, if different from Report)*

18. SUPPLEMENTARY NOTES

DTIC ELECTE JAN 14 1981 S D

19. KEY WORDS *(Continue on reverse side if necessary and identify by block number)*

LORAN-C

20. ABSTRACT *(Continue on reverse side if necessary and identify by block number)*

LORAN-C reliability diagrams produced at the Defense Mapping Agency Hydrographic/Topographic Center depict two types of data: ~~(a)~~ the maximum usable groundwave signal limit, which aids the LORAN-C user in determining which transmitters provide coverage in his area of operation, and ~~(b)~~ the predicted uncertainty of a LORAN-C hyperbolic fix.

Signal limits are computed using Bremmer's field prediction formula (~~Ref. 1~~) and an algorithm that predicts the range for a signal of predetermined signal-to-noise-

DD FORM 1 JAN 73 1473 EDITION OF 1 NOV 65 IS OBSOLETE

UNCLASSIFIED

SECURITY CLASSIFICATION OF THIS PAGE (When Data Entered)

AD A093749

DDC FILE COPY

81 1 13 035

ratio propagating along an electrically inhomogeneous transmission path (Ref. 2). Fix uncertainty predictions are based on a formula relating fix uncertainty to (a) crossing angle between lines of position, (b) system standard deviation, and (c) the divergence of hyperbolic lines of position.

Actual range and fix undertainty may differ from values shown on reliability diagrams, depending on such factors as weather, the occurrence of geomagnetic disturbances, and the user's direction of travel.

Reliability diagrams currently produced show signal limits and fix uncertainties for LORAN-C chains at a scale of 1:5,000,000; a new generation of reliability diagrams could show data at a reduced scale (1:10,000,000) for each LORAN-C triad (one master and two slave transmitters), making more chain and transmitter selection information available to the user.

References Cited in Abstract

(1) J. R. Johler, W. J. Kellar, and L. C. Walters.
Phase of the low radiofrequency ground wave.
National Bureau of Standards Circular 573, 1956.

(2) C. L. Worrell.
Production of LORAN-C reliability diagrams:
Computation of the maximum usable groundwave signal limit.
In preparation.

PRODUCTION OF LORAN-C RELIABILITY DIAGRAMS AT THE DEFENSE MAPPING AGENCY

by

Clarence L. Worrell
Electronic Navigation Division
Defense Mapping Agency
Hydrographic/Topographic Center
6500 Brookes Lane Washington, D.C. 20315

Mr. Worrell, a navigational scientist with the DMA, received his B.S. degree in geophysics from Virginia Tech in 1977. Prior to joining DMA, Mr. Worrell worked with Western Geophysical Company in Houston, Texas.

ABSTRACT

LORAN-C reliability diagrams produced at the Defense Mapping Agency Hydrographic/Topographic Center depict two types of data: (a) the maximum usable groundwave signal limit, which aids the LORAN-C user in determining which transmitters provide coverage in his area of operation, and (b) the predicted uncertainty of a LORAN-C hyperbolic fix.

Signal limits are computed using Bremmer's field prediction formula (Ref. 1) and an algorithm that predicts the range for a signal of predetermined signal-to-noise ratio propagating along an electrically inhomogeneous transmission path (Ref. 2). Fix uncertainty predictions are based on a formula relating fix uncertainty to (a) crossing angle between lines of position, (b) system standard deviation, and (c) the divergence of hyperbolic lines of position.

Actual range and fix uncertainty may differ from values shown on reliability diagrams, depending on such factors as weather, the occurrence of geomagnetic disturbances, and the user's direction of travel.

Reliability diagrams currently produced show signal limits and fix uncertainties for LORAN-C chains at a scale of 1:5,000,000; a new generation of reliability diagrams could show data at a reduced scale (1:10,000,000) for each LORAN-C triad (one master and two slave transmitters), making more chain and transmitter selection information available to the user.

INTRODUCTION

The LORAN-C Navigation System

LORAN-C is a pulsed, low frequency (100 kHz) electronic navigation system operated by the U.S. Coast Guard. LORAN-C provides fix data to vessels operating in the northern, northwestern, and central Pacific, the Mediterranean, the northern Atlantic, and the U.S. Coastal Confluence Zone.

LORAN-C is operable in either of two modes: (a) range-range mode, in which a fix is defined by the intersection of two circular lines of positions (LOP's) defined by the arrival times of LORAN-C pulses from two synchronized transmitters, and (b) hyperbolic mode, in which each LOP is hyperbolic and is defined by the difference in arrival times of pulses from two synchronized transmitters.

Synchronization of LORAN-C transmissions is maintained by system area monitors which record, at fixed positions, time differences (TD's) in pulse arrivals from each master-slave transmitter pair operating in the area. If TD's measured at a monitor drift excessively from the norm, then the monitor directs the slave transmitter to make a change in pulse timing to compensate for the drift.

The ideas expressed in this paper represent the opinions of the author and do not necessarily reflect official policies of the DMA.

A LORAN-C chain consists of one master transmitter (which initiates the transmission of pulses from other transmitters in the chain) and several secondary (or slave) transmitters; each LORAN-C chain is assigned a unique group repetition interval (GRI). The GRI is the length, commonly expressed in tens of microseconds, of the coded sequence of pulses that comprise the LORAN-C signal format.

General Description of the LORAN-C Reliability Diagram

Shown in Fig. 1 is the LORAN-C reliability diagram for the Gulf of Mexico (GRI 7980). (A list of the currently available LORAN-C reliability and coverage diagrams is in Appendix A.)

Two types of data, depicted on a Lambert conformal conic projection of land-sea interfaces at a scale of 1:5,000,000, are shown in the diagram: (a) the maximum usable groundwave signal limits for signal-to-noise ratios (SNR's) of 1:3 and 1:10 and (b) predicted fix uncertainty.

The signal limit contours define the areas in which the LORAN-C groundwave signal from each transmitter in the chain is of sufficient field strength to be detected by either commercially available receivers (generally capable of extracting signal at SNR's of at least 1:3) or military receivers (generally capable of extracting signal at SNR's of at least 1:10).

Predicted fix uncertainty contours define the areas in which the accuracy of the LORAN-C system, operating in hyperbolic mode, is limited by random errors such as those caused by transmitter instability or variable radiowave propagation conditions. Contours representing fix uncertainties of 500, 750, and 1500 ft. are shown in reliability diagrams.

The information shown in reliability diagrams aids the LORAN-C user both in (a) planning chain and transmitter selection for a voyage and (b) making enroute changes in chain and transmitter selection that become necessary when a transmitter's signal becomes unusable due to conditions such as transmitter failure or changes in weather.

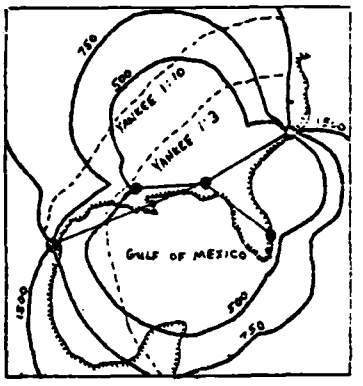

Figure 1. LORAN-C reliability diagram for the Gulf of Mexico (GRI 7980). (Signal limits for the master transmitter and for slaves W, X, and Z are not shown.)

PREDICTING THE MAXIMUM USABLE GROUNDWAVE SIGNAL LIMIT

Attenuation of the LORAN-C Signal

The LORAN-C signal loses energy as it is transmitted along the earth's surface; this loss results from signal front spreading, energy scattering by irregular terrain, energy absorption by the earth and its atmosphere, etc. Factors such as transmission path characteristics, transmitted power, and distance traveled by the signal affect the amount of energy lost by that signal. Transmission path characteristics include (a) physical properties, such as curvature of the earth's surface, and (b) electrical properties (ground conductivity and permittivity, atmospheric refractivity) which vary as functions of weather (Ref. 3), vegetation, and terrain ruggedness.

LORAN-C receivers are designed to sample the LORAN-C pulse 25 microseconds (usec) following its leading edge; this standard sampling point (SSP) occurs, ideally, at 0.506 of the pulse's peak amplitude (Ref. 4). See Fig. 2. For purposes of predicting field strength, the signal level of the LORAN-C pulse is taken to be the root-mean-square (rms) amplitude of a continuous wave whose amplitude is that of the pulse at its SSP (Fig. 2).

At some distance along its transmission path, the groundwave component of the LORAN-C pulse loses so much energy that it becomes indistinguishable from the ambient atmospheric noise. This occurs generally at a SNR of 1:3 for commercial receivers or 1:10 for military receivers. The SNR is the ratio of the LORAN-C signal's field strength at 0.128 of its peak power to the rms field strength of the ambient atmospheric noise, as determined from CCIR report 322 (Refs. 5, 6).

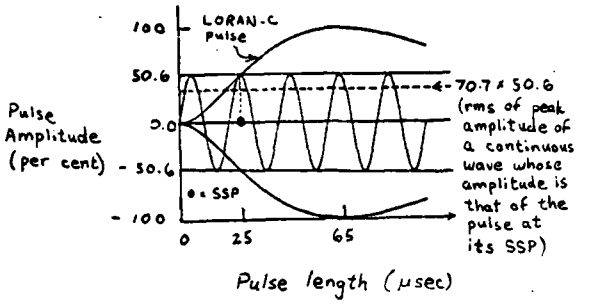

Figure 2. The LORAN-C pulse is sampled 25 usec after it begins. The signal level of the pulse is defined as 0.707 of 0.506 of the pulse's peak amplitude (0.128 of its peak power).

Procedure for Predicting Signal Limits Shown on Reliability Diagrams

(Step 1)

A number of azimuths radiating outward from each transmitter in a LORAN-C chain are chosen. Each azimuth represents an electrically inhomogeneous transmission path, and is treated as a "mixed path" consisting of a number of electrically homogeneous terrain segments. The electrical properties of some common terrain types are shown in Table 1.

Table 1

Type of Surface	Conductivity (mhos/meter)	Permittivity (relative to free space)
Sea water	3 to 5	80
Rich, damp soils, not heavily leached	10^{-2} to 3×10^{-2}	15 to 30
Dry sandy soils, or heavily leached areas	10^{-3}	10 to 20
Very thin soil, over rock	10^{-4} to 10^{-3}	5 to 10
Fresh water, average lake	10^{-3} to 3×10^{-3}	80
Glacial ice	4×10^{-5}	10 to 20

(Taken from Ref. 7)

The division of an azimuth into homogeneous terrain segments is based on maps of either conductivity boundaries or land-sea interfaces. (Shown in Ref. 8 is a map of conductivities for the United States.)

(Step 2)

Once the average ambient atmospheric noise level for the area surrounding a transmitter is established, the field strengths of the LORAN-C signal at SNR's of 1:3 and 1:10 are calculated. Using field strength curves, such as the one in Fig. 3, the signal limit of each type of terrain segment is determined.

Field strength curves are computed using Bremmer's far field prediction formula (Appendix B).

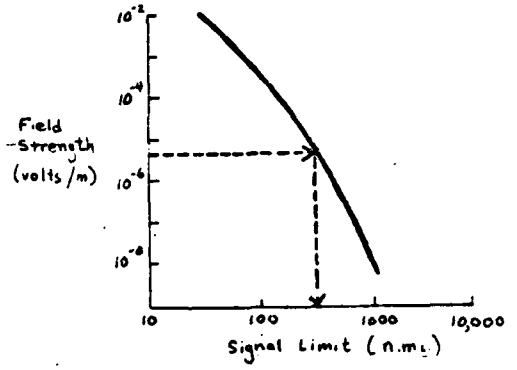

Figure 3. The signal limit for each type of terrain segment is determined using field strength curves based on Bremmer's formula. In this example, the limit for a signal of field strength 6×10^{-6} volt/meter is 420 nautical miles.

(Step 3)

Once the signal limit for each type of terrain segment is predicted, the signal limit of the inhomogeneous transmission path can be predicted using the method derived below (Ref. 2).

Shown in Fig. 4 is a mixed-path approximation of an inhomogeneous transmission path. The segment lenghts are labeled L(i,j); the segments are numbered, outward from the transmitter, i=1, i=2, ... , i=n for terrain types j=1, j=2, ... , j=m.

Having predicted the signal limits S(j) for each terrain type and S (sea) for an all sea water path, a sea-equivalency factor F(j) is defined:

$$F(j)=S(sea)/S(j) \qquad \text{(Eq. 1)}$$

Each terrain segment of length L(i,j) can be converted to a sea-equivalent segment of length G(i) using the relation

$$G(i)=F(j)\ X\ L(i,j) \qquad \text{(Eq. 2}$$

(The length G(i) is the distance a signal would travel over sea water before attenuating to the level it would attenuate to by traveling a distance L(i,j) over terrain of type j.)

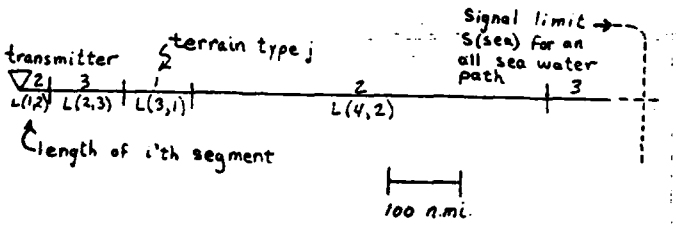

Figure 4. Mixed-path approximation of an inhomogeneous transmission path.

Applying Eq. 2 converts a mixed-terrain transmission path to an all sea water transmission path. The sea water signal limit S(sea) is known, so the mixed-path signal limit can be calculated by converting all sea-equivalent segments up to S(sea) back to terrain segments, then summing their lengths:

$$\sum_{i=1}^{A} G(i) = S(sea) \qquad \text{(Eq. 3)}$$

where the A'th sea-equivalent segment extends to S(sea).

If the A'th segment "straddles" S(sea), in other words,

$$\text{if} \quad \sum_{i=1}^{A} G(i) > S(sea) \qquad \text{(Eq. 4)}$$

and $\sum_{i=1}^{A-1} G(i) < S(sea)$ (Eq. 5)

then Eq. 3 must be modified.

That part of the A'th sea-equivalent segment that lies within S(sea) is the residual

$$RES = S(sea) - \sum_{i=1}^{A-1} G(i) \quad \text{(Eq. 6)}$$

The mixed-path signal limit S(mixed) is predicted by converting the sea-equivalent segments G(1) through G(A-1) and RES back to their original lengths L(i,j) and r, and summing:

$$S(mixed) = \sum_{i=1}^{A-1} L(i,j) + r \quad \text{(Eq. 7)}$$

where $r = RES/F(j)_A$ (Eq. 8)

$(F(j)A = F(j)$ for $i=A)$.

Thus,

$$S(mixed) = \sum_{i=1}^{A-1} L(i,j) + \frac{S(sea) - \sum_{i=1}^{A-1} F(j) L(i,j)}{F(j)_A} \quad \text{(Eq. 9)}$$

$$= \frac{S(sea) + \sum_{i=1}^{A-1} [F(j)_A - F(j)] L(i,j)}{F(j)_A} \quad \text{(Eq. 10)}$$

As an example, refer to Tables 2 and 3. In Table 2 are predicted signal limits and sea-equivalency factors for three terrain types; in Table 3 are sea-equivalent lengths G(i) calculated for each of five segments in a mixed-terrain transmission path. (Note that the fourth terrain segment straddles S(sea), hence A=4.) Using Eq. 10, the mixed-path signal limit is calculated to be 353 nautical miles (n.mi.). This technique for predicting mixed-path signal limits is represented graphically in Fig. 5.

Table 2

Terrain Type (j)	Sea-Equivalency factor F(j)	Signal Limit S(j) (n.mi.)
1	1.1	810
2	4.5	200
3	1.0	900

Note: S(sea) = S(3).

Table 3

Terrain Segment i	Terrain Type j	Segment Length L(i,j) (n.mi.)	Sea-Equivalent Length G(i) (n.mi.)
1	2	50	225
2	3	100	100
3	1	100	110
4	2	500	2250
5	3	600	600

Note: RES = 900-(225+100+110) = 465 n.mi.

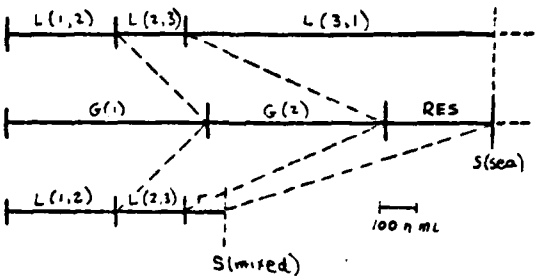

Figure 5. Prediction of mixed-path signal limits shown on reliability diagrams: (1) approximate inhomogeneous transmission path as a mixed-path, (2) convert terrain segments to sea-equivalent segments and determine length of residual RES, and (3) convert sea-equivalent segments and RES back to terrain segments (Ref. 2).

(Step 4)

For each azimuth (transmission path) radiating outward from a given transmitter, predicted signal limits for SNR's of 1:3 and 1:10 are plotted, then contoured.

Other Methods of Predicting Mixed-Path Signal Limits

Using Eq. 10 to predict signal limits requires much less computer time than other known methods, such as Millington's (Refs. 9-12). Millington's method of predicting the field strength of a groundwave transmitted over a mixed-terrain path is given by

$$E(d_1+d_2+\ldots+d_n) = \left\{ E_1(d_1) \frac{E_2(d_1+d_2)}{E_2(d_1)} \cdots \frac{E_n(d_1+d_2+\ldots+d_n)}{E_n(d_1+\ldots+d_{n-1})} \right.$$

$$\left. \times E_n(d_n) \frac{E_{n-1}(d_{n-1}+d_n)}{E_{n-1}(d_n)} \cdots \frac{E_1(d_1+d_2+\ldots+d_n)}{E_1(d_n+d_{n-1}+\ldots+d_2)} \right\}^{\frac{1}{2}} \quad \text{(Eq. 11)}$$

where $E_j(d_k)$ is the field strength of a groundwave transmitted a distance d_k over a terrain of type j.

To predict a signal limit using Millington's method, Eq. 11 must be solved for a range of transmitter-to-receiver distances to determine at what distance the signal attenuates to its 1:3 or 1:10 SNR level.

Signal limits predicted using Eq. 10 were within 14% of the limits predicted using Millington's method in 17 of the 20 representative mixed-paths tested. Eq. 10 produced signal limit predictions that were, on the average, 11% more pessimistic than those produced by Millington's method.

Eq. 10 does not take into account the fact that a signal's attenuation rate (in decibels/100 n.mi., for instance) decreases with distance from the transmitter at different rates for different kinds of terrain. The effect this has on computing sea-equivalent segments is shown in Table 4: a terrain segment has a sea-equivalent segment whose length varies with distance from the transmitter. One method of predicting attenuation over a mixed path that accounts for the effects of the variable attenuation rate is described below (Ref. 14).

Consider the terrain segments described in Tables 2 and 3. Using the set of field strength curves in Fig. 6, the attenuation (in decibels, dB) of a signal propagating over terrain type 2 between 0 and 50 n.mi. from its transmitter is determined. Next, the attenuation of a signal propagating between 50 and 150 n.mi. is determined, and so on. The total attenuation over a distance d is the sum of the attenuation values (in dB) of all segments up to distance d.

Table 4

Terrain Segment	Attenuation of Signal Transmitted Across Terrain Segment *	Sea-Equivalent Segment **
1 to 101 km	41 dB	1 to 115 km
400 to 500	3.5	400 to 520
1000 to 1100	2.5	1000 to 1150

* assuming permittivity (relative to free space) is 15 and conductivity is 10^{-3} mho/meter.

** sea-equivalent segment length determined for the attenuation given in column two.

Data taken from Ref. 13.

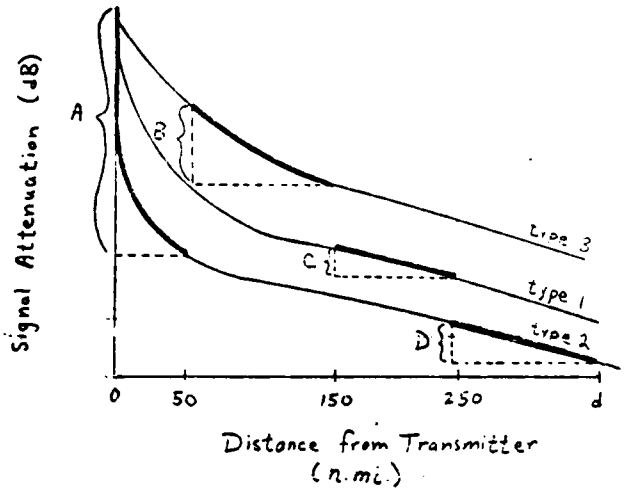

Figure 6. The total attenuation over the mixed path from 0 to d is A+B+C+D decibels.

PREDICTION OF LORAN-C FIX UNCERTAINTY

Definition of Fix Uncertainty

A LORAN-C position fix is defined by the intersection of two hyperbolic LOP's. Due to factors such as transmitter instability and variable propagation conditions, the geographic location of each LOP changes with time; this variation is essentially random and is assumed to occur as a normal distribution. The location of the intersection of two LOP's is thus assumed to vary as a two-dimensional normal distribution.

Fix uncertainty contours depicted on LORAN-C reliability diagrams show area in which a fix has a 95% chance of being within 1500, 750, or 500 ft. of the center of this two-dimensional normal distribution, barring the occurrence of non-random errors. (The center of the distribution may or may not be associated with a distinct geodetic position.)

As an example, consider a LORAN-C receiver, located at a stationary position within the area defined by the 500 ft. uncertainty contour, monitoring TD's for several weeks. 95% of the position fixes defined by these TD's will be within 500 ft. of the stationary receiver.

Fix uncertainty due to the random instability in LOP location increases as the crossing angle between LOP's decreases (Fig. 7). In addition, fix uncertainty increases as hyperbolic LOP's diverge. For example, a TD error of 0.1 usec along the baseline between a master and a slave transmitter corresponds to a distance error of about 50 ft.; near the baseline extension, where LOP's are highly divergent, the same TD error represents a distance error of several hundred feet (Fig. 8).

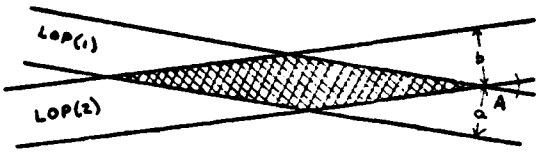

Figure 7. Fix undertainty due to LOP instability over distances a and b is exaggerated by the small crossing angle A.

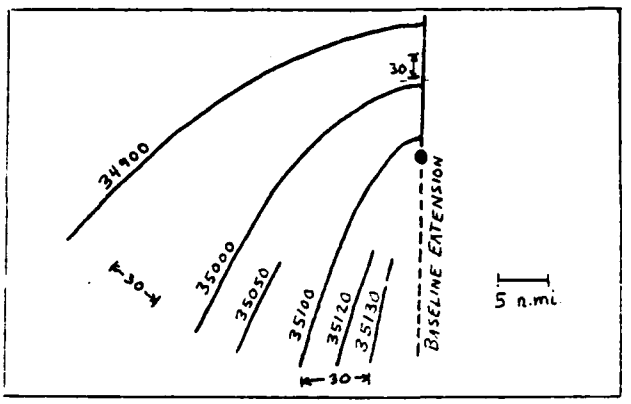

Figure 8. Hyperbolic LOP's (labeled in microseconds of time difference) diverging away from the baseline.

Thus, fix uncertainty contours show areas in which the accuracy of the LORAN-C system is limited by the random instability of hyperbolic position lines. Fix uncertainty due to this instability is amplified (a) where crossing angles between LOP's are small and (b) where LOP's diverge.

Fix uncertainty must not be confused with "absolute accuracy" - the accuracy with which a LORAN-C fix can be associated with a distinct geodetic position. The absolute accuracy of a LORAN-C fix is a function of both (a) fix uncertainty and (b) the ability to correctly predict the time required for a LORAN-C signal to propagate from its transmitter to any given geodetic position.

Fix uncertainty is similar to repeatable accuracy (the accuracy with which a vessel can return to a previous position using LORAN-C). In an area of 500 ft. repeatable accuracy, a vessel, using the same LORAN-C TD coordinates, can return to the same position repeatedly to within 500 ft., most of the time.

In an area of 500 ft. fix uncertainty, a vessel will be able to position itself to within 500 ft. of a buoy using the TD coordinates of that buoy, provided these TD coordinates have been established by monitoring TD's at the buoy for a sufficient length of time.

Derivation of an Approximate Method for Predicting Fix Uncertainty

Fix uncertainty data depicted on LORAN-C reliability diagrams are computed using a formula derived by Trow and Jessell (Ref. 15). A similar formula is derived by Sitterly (Ref. 16). This formula defines the "95 percent radial error" - the radius of the circle containing about 95% of all fixes associated with a given TD pair.

Shown in Fig. 9 are two LOP's intersecting at an angle A and displaced from their average positions by random errors e(1) and e(2). The major diagonal d of the parallelogram thus formed is the position fix error associated with random errors e (1) and e(2). d can be expressed, according to the Law of Cosines, as

$$d^2 = p^2 + q^2 + 2pq \cos A \qquad \text{(Eq. 12)}$$

(p and q are the lengths of the parallelograms sides).

By the definition of sine,

$$p = \frac{e(1)}{\sin A} \quad , \quad q = \frac{e(2)}{\sin A} \qquad \text{(Eq. 13).}$$

Combining Eqs. 12 and 13 gives

$$d^2 = \left(\frac{e(1)}{\sin A}\right)^2 + \left(\frac{e(2)}{\sin A}\right)^2 + \frac{2\,e(1)\,e(2)\cos A}{\sin^2 A} \qquad \text{(Eq. 14)}$$

Eq. 14 relates position fix error d to (a) random variations that occur in LOP location and (b) LOP crossing angle. The magnitudes of roughly 95% of these position fix errors are smaller than twice their root mean square (twice their standard deviation) 2drms. (This approximation is made assuming that the fix error d is normally distributed, which it is not; the probability that d is smaller than 2drms varies with the crossing angle.) Thus, fix uncertainty is approximated as

$$95\%\ \text{radial error} \approx 2\text{drms} = 2\sqrt{\tfrac{1}{n}\Sigma d^2} \qquad \text{(Eq. 15).}$$

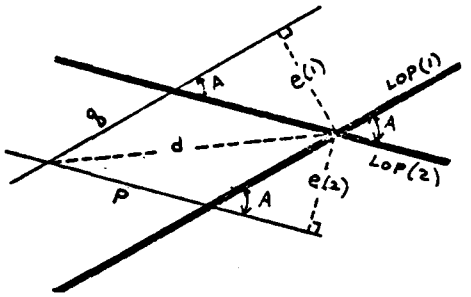

Figure 9. d is the position fix error associated with random errors e(1) and e(2).

Substituting from Eq. 14, Eq. 15 becomes

$$2\text{drms} = 2\left\{\frac{1}{n}\Sigma\left(\frac{e(1)}{\sin A}\right)^2 + \frac{1}{n}\Sigma\left(\frac{e(2)}{\sin A}\right)^2 + \frac{1}{n}\Sigma\frac{e(1)e(2)\cos A}{\sin^2 A}\right\}^{1/2} \qquad \text{(Eq. 16).}$$

Recalling that the standard deviation of a normal distribution of errors is

$$sd = \sqrt{\tfrac{1}{n}\Sigma e^2} \qquad \text{(Eq. 17)}$$

and letting the "correlation coefficient" be defined as

$$C = \frac{\Sigma e(1)\,e(2)}{n\sqrt{\frac{1}{n}\left(\frac{e(1)}{\sin A}\right)^2}\sqrt{\frac{1}{n}\left(\frac{e(2)}{\sin A}\right)^2}} \qquad \text{(Eq. 18),}$$

Eq. 16 becomes

$$2\text{drms} = \frac{2}{\sin A}\left(sd(1)^2 + sd(2)^2 + 2\,sd(1)\,sd(2)\,C\cos A\right)^{1/2} \qquad \text{(Eq. 19).}$$

The correlation coefficient C varies between -1 and 1, indicating the degree to which random errors e(1) and e(2) are related to one another by some common causal mechanism.

The standard deviations sd(1) and sd(2) in LOP location should be expressed in a way that reflects the effects of LOP divergence. Shown in Fig. 10 are two ray path distances r(1) and r(2) between each of two transmitters and a LORAN-C receiver (located at R). Also shown is the line segment tangent to the hyperbolic LOP at R. This segment bisects the angle 2B between ray paths r(1) and r(2). Because of instability, the LOP at R may be displaced a distance DISP to R'; DISP can be approximately expressed in terms of a variation dr in ray path lengths r(1) and r(2):

$$DISP = dr / \sin B \qquad \text{(Eq. 20)}$$

The hyperbolic position line at R is defined by

$$r(1) - r(2) = \text{constant} \qquad \text{(Eq. 21).}$$

So the displaced LOP at R' is defined by

$$(r(1)+dr)-(r(2)-dr) = r(1)-r(2)+2dr = \text{constant} \qquad \text{(Eq. 22)}$$

The distance 2dr can be expressed as a time difference error dt:

$$dt = 2dr/c \qquad \text{(Eq. 23)}$$

where c is the speed of light through the atmosphere.

Combining Eqs. 20 and 23 gives

$$DISP = \frac{1/2\ dt \cdot c}{\sin B} \qquad \text{(Eq. 24).}$$

Letting DISP be a random error in LOP location (such as e(1) or e(2) in Fig. 9) the standard deviation sd becomes

$$sd = \sqrt{\tfrac{1}{n}\Sigma DISP^2} = \frac{1/2\,c}{\sin B}\sqrt{\tfrac{1}{n}\Sigma dt^2} = \frac{1/2\,sdt\cdot c}{\sin B} \qquad \text{(Eq. 25)}$$

where sdt is the standard deviation of random time difference errors (also called the "system standard deviation").

Thus, assuming no correlation in random errors (C=0), Eq. 19 (which approximates fix uncertainty) reduces to

$$2\text{drms} = \frac{sdt\cdot c}{\sin A}\left\{\left(\frac{1}{\sin B(1)}\right)^2 + \left(\frac{1}{\sin B(2)}\right)^2\right\}^{1/2} \qquad \text{(Eq. 26).}$$

(1/sinB(1) and 1/sinB(2) are often called "expansion factors" or "position line divergence factors".)

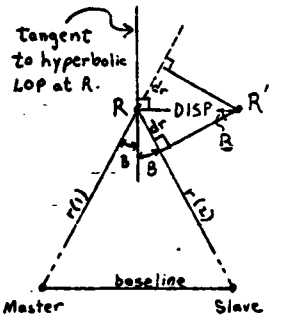

Figure 10. The displacement DISP of an LOP can be expressed approximately in terms of the deviations dr in raypath lengths r(1) and r(2). (Taken from Ref. 15.)

Fix Uncertainty Contours

For a LORAN-C triad, the crossing angle A is the sum (or difference) of angles B(1) and B(2), as shown in Fig. 11. Thus, for a given location relative to the LORAN-C triad, the fix uncertainty 2drms can be computed using Eq. 26.

Fix uncertainty contours shown on LORAN-C reliability diagrams are derived by first solving Eq. 26 for each node in a spheroidal grid of latitudes and longitudes in the vicinity of the LORAN-C triad. Next, an interpolation scheme is used to determine the geographic coordinates for contours of 1500, 750, and 500 ft. fix uncertainty. These coordinates are plotted, using a Lambert conformal conic projection, for each triad in a LORAN-C chain; the resulting fix uncertainty plots are composited for the entire LORAN-C chain.

It is assumed in these computations that the standard deviation of TD errors sdt is 0.1 usec.

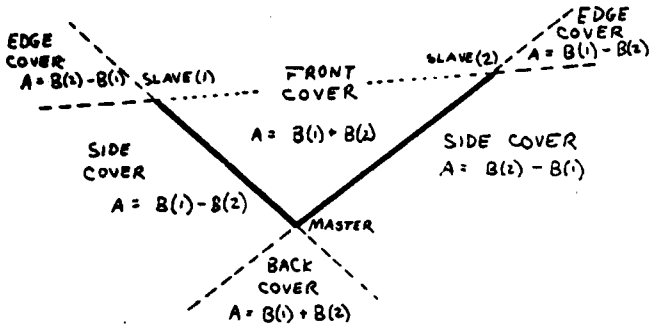

Figure 11. Crossing angle A is the sum (or difference) in bisecting angles B(1) and B(2). (Taken from Ref. 15.)

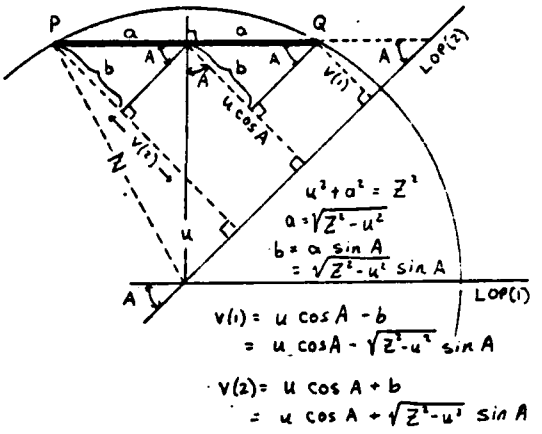

Figure 12. The probability that a position fix, defined by LOP(1) and LOP(2), will fall within the very thin parallelogram PQ is given by Eq. 28 where v(1) and v(2) are defined as above.

A More Exact Method of Predicting Fix Uncertainty

The error d due to random variations in LOP location does not occur as a normal distribution. The actual distribution of errors is described by the relation

$$95\%\ \text{radial error} = K d_{rms} = K\sqrt{\frac{1}{n}\Sigma d^2} \quad \text{(eq. 27)}$$

where K varies between about 1.73 and 1.96 as a function of the crossing angle and the ratio sd(1)/sd(2). Approximating the 95% radial error as 2.00 drms thus produces a pessimistic prediction of fix uncertainty.

In an approach desribed by Sitterly (Ref. 16) and investigated in detail by Hiraiwa (Refs. 17, 18) the coefficient K is computed; this two-part process is described below.

(Step 1)

Shown in Fig. 12 are two LOP's intersecting at an angle A. The probability that a position fix, associated with the intersection of LOP(1) and LOP(2), will fall within the very thin parallelogram PQ is given by

$$\text{probability} = \frac{1}{2\pi\, sd(1)\, sd(2)} \int_{u(1)}^{u(2)} \exp\left(\frac{-u^2}{2\,sd(1)^2}\right) du \int_{v(1)}^{v(2)} \exp\left(\frac{-v^2}{2\,sd(2)^2}\right) dv \quad \text{(Eq. 28).}$$

sd(1) and sd(2) are the standard deviations of LOP(1) and LOP(2) from their average locations. du is the thickness of PQ in the direction perpendicular to LOP(1). Lengths v(1) and v(2) are perpendicular to LOP(2) and define the points P and Q. As shown in Fig. 12, v(1) and v(2) are defined, in terms of perpendicular distance u from LOP(1), as

$$v(1) = u \cos A + \sqrt{Z^2 - u^2}\, \sin A \quad \text{(Eq. 29)}$$

$$v(2) = u \cos A - \sqrt{Z^2 - u^2}\, \sin A \quad \text{(Eq. 30).}$$

The probability that a position fix lies within a circle of radius Z can thus be computed using Eqs. 28-30, numerically integrating over the interval u(1)=0, u(2)=Z, and multiplying the results by 2. This is done for various values of Z, sd(1)/sd(2), and crossing angle A to determine which combinations of these values produce a probability of 95%.

(Step 2)

Using the same steps by which Eq. 19 is derived, Eq. 27 becomes (for C=0)

$$Z \triangleq 95\%\ \text{radial error} = \frac{K}{\sin A}\sqrt{sd(1)^2 + sd(2)^2} \quad \text{(Eq. 31).}$$

Eq. 31 is solved for K using the various values of Z, sd(1)/sd(2), and A determined in Step 1. Shown in Fig. 13 is a graph of K as a function of sd(1)/sd(2) and A.

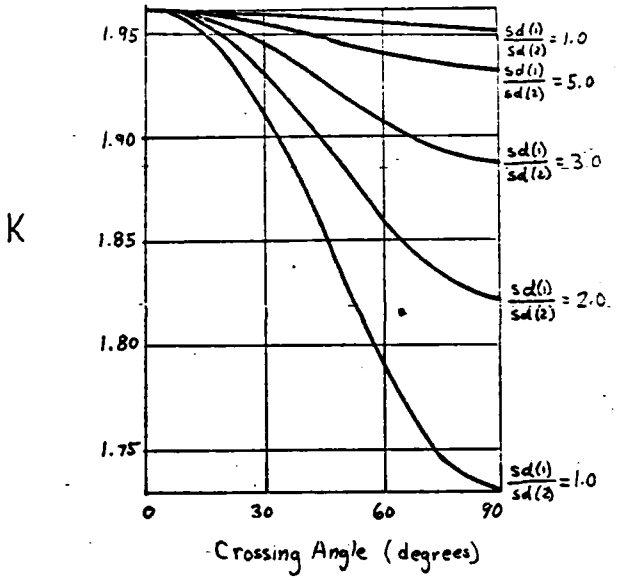

Figure 13. Graph of K as a function of crossing angle and the ratio sd(1)/sd(2). (Taken from Ref. 17.)

Having determined K, the "true" 95% radial error is computed as

$$K d_{rms} = \frac{1/2\, k\, sdt \cdot c}{\sin A}\left\{\left(\frac{1}{\sin B(1)}\right)^2 + \left(\frac{1}{\sin B(2)}\right)^2\right\}^{1/2} \quad \text{(Eq 32)}$$

(See Eq. 26).

A comparison of fix uncertainty values computed using Kdrms with those computed using 2drms is shown in Fig. 14.

Reliability diagrams produced in the future by DMA may depict fix uncertainty data computed using Kdrms.

PRESENTATION OF DATA

Reliability Diagrams

Fix uncertainty and signal limit data are plotted for each LORAN-C chain on a 1:5,000,000 Lambert conformal conic projection of land-sea interfaces. No signal limits are shown outside the 1500 ft. fix uncertainty contour.

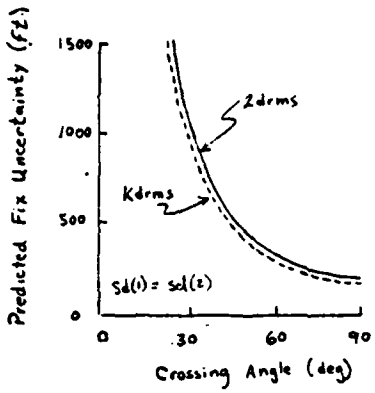

Figure 14. Comparison of fix uncertainty values computed as Kdrms with those computed as 2drms; note that the difference is most significant for small crossing angles.

Coverage Diagrams

LORAN-C coverage diagrams show contours of skywave and groundwave coverage. Groundwave coverage contours define areas in which these conditions exist:

(a) predicted fix uncertainty is 1500 ft. or less, and
(b) predicted groundwave signal strength exceeds a 1:3 SNR.

Triad Diagrams

It is often impossible, using currently available reliability diagrams, to determine fix uncertainty for a given triad within a LORAN-C chain. For example, the dark solid line in Fig. 15 is the 750 ft. fix uncertainty contour for the chain MXYZ. Using this chain diagram, a user operating in the shaded area, using TD's from the MXY triad, cannot determine fix uncertainty. A triad diagram for transmitters M, X, and Y reveals the location of the 750 ft. contour (dashed line in Fig. 15).

Four triad diagrams, each at a scale of 1:10,000,000, can be printed on the same size sheet as one of the currently available reliability diagrams.

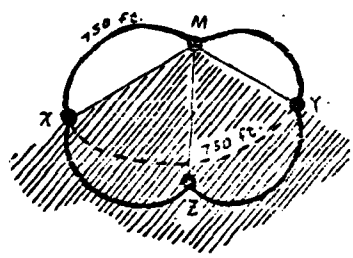

Figure 15. 750 ft. fix uncertainty contour (dark solid line) for the MXYZ chain. A user operating in the shaded area, using TD's from the MXY triad, cannot determine fix uncertainty using this diagram.

Absolute Accuracy

In areas where LORAN-C data are controlled by high quality data from systems such as NNSS (Transit satellite) or Autotape, accuracy information could be depicted in reliability diagrams, possibly as shading in various tones of gray.

DIFFICULTIES AND IMPOSSIBILITIES IN PREDICTING SIGNAL LIMITS AND FIX UNCERTAINTIES

Actual signal limits and fix uncertainties often differ from predicted values, due to a variety of causes, including:

(a) our inability to predict either the occurrence, or the effects on signal propagation, of non-periodic phenomena such as thunderstorms and geomagnetic disturbances;
(b) our inability to accurately predict the effects of periodic phenomena, such as seasonal climate changes, on signal propagation;
(c) Inaccuracies in predictions of noise level, groundwave field strength, and fix uncertainty due to assumptions made in the predition models (for example, the system standard deviation will differ from the assumed 0.1 usec, depending on the propagation conditions that exist at a given moment);
(d) limitations in availability and accuracy of data, such as ground conductivities, used in the prediction models.

In addition, variables such as the user's direction of travel affect signal limits and fix uncertainties observed by the user (a LORAN-C receiver may "lock on" to a signal close to the transmitter and track that signal far beyond its predicted limit).

In an effort to make reliability diagrams as accurate and useful as possible, I make the following recommendations:

(a) use the method described in Fig. 6 to predict groundwave signal limits;
(b) use Hiraiwa's method (Eq. 32) to predict fix uncertainty;
(c) present fix uncertainty and signal limit data for single triads, rather than for entire chains;
(d) where data are available, show absolute accuracy information on reliability diagrams.

APPENDIX A. CURRENTLY AVAILABLE LORAN-C COVERAGE AND RELIABILITY DIAGRAMS

DMA Stock Number	Area (GRI)
WOBZP5130	LORAN-C Coverage Diagram
WOBZP5131	LORAN-A Coverage Diagram

Reliability Diagrams:

ZLORX5592	Mediterranean Sea (7990)
ZLORX5593	Norwegian Sea (7970)
ZLORX5595	North Pacific (9990)
ZLORX5596	Central Pacific (4990)
ZLORX5597	Northwest Pacific (9970)
ZLORX5598	North Atlantic (7930)
ZLORX5600	Gulf of Alaska (7960)
ZLORX5601	Canadian West Coast (5990)
ZLORX5602	West Coast, U.S.A. (9940)
ZLORX5603	Southeast U.S.A. (7980)
ZLORX5604	Northeast U.S.A. 99960)
ZLORX5605	Great Lakes (8970)

These diagrams are available through agents of the DMA Office of Distribution Services; addresses of these agents are listed in the Defense Mapping Agency Catalogue of Maps, Charts, and Related Products (Publication 1-N-L, DMA stock number CATALNL).

APPENDIX B. BREMMER'S FAR FIELD PREDICTION FORMULA

Bremmer's formula (Refs. 1, 9, 10, 19, 20, 21, 22) is used to predict the vertical field of a groundwave propagating along a smooth, spherical, electrically homogeneous earth. The strength of this field (in volts/meter) is calculated as

$$|Er| = (E(R)^2 + E(I)^2)^{\frac{1}{2}} \qquad \text{(Eq. 33)}$$

where E(R) and E(I) are the real and imaginary components of the groundwave field.

Eq. 34 is Bremmer's formula, below which are defined the terms used in the formula.

$$E_r = \left[\frac{-2i\,I_{ol}\,k_1^2\,e^{ik_1 d}}{4\pi\epsilon_1\omega d}\right]\left[2\pi(k_1 a_e)^{1/3}\left(\frac{d}{a_e}\right)\right]^{1/2} \times \sum_{s=0}^{\infty} \frac{e^{i\left((k_1 a_e)^{1/3}\tau_s \frac{d}{a_e} + \frac{d}{2a_e} + \frac{\pi}{4}\right)}}{2\tau_s - 1/\delta^2} \qquad \text{(Eq. 34)}$$

Er = vertical electrical field (volts/meter), both transmitter and receiver on the ground.

$i = \sqrt{-1}$

Iol = dipole moment of source (amp-meters). Computations can be made assuming Iol = 1, then the results scaled up according to the relationship (Ref. 23) Er = $0.3\sqrt{P}$ volts/meter at 1 km (0.54 n.mi.) from the transmitter. P is 0.128 of the peak transmitted power in kilowatts.

$K_1 = \frac{\omega}{c_o}\sqrt{\frac{\epsilon_1}{\epsilon_o}}$ = wave number of the atmosphere (radians/meter).

$\omega = 2\pi f$ = radial frequency of transmitted signal.

f = linear frequency of the transmitted signal. No more than 1% of the radiated energy in a LORAN-C signal lies outside the 90-110 kHz band (Ref. 24).

c_o = speed of light in free space = 2.99792458×10^8 meters/second.

$\sqrt{\frac{\epsilon_1}{\epsilon_o}}$ = index of refraction of the atmosphere = 1.000338 at the earth's surface for a standard atmosphere. $\sqrt{\frac{\epsilon_1}{\epsilon_o}}$ varies as a function of weather.

ϵ_1 = permittivity of the atmosphere.

ϵ_o = permittivity of free space = 8.85×10^{-12} farad/meter. Permittivity is the measure of electrical "transparency" of a propagation medium.

d = distance travelled by signal. Eq. 34 is useful for d > 80 km for LORAN-C frequency.

a_e = effective radius of earth = 4/3 of radius of a spherical earth. a_e is used in Eq. 34 to compensate, in part, for the effects of an inhomogeneous atmosphere.

each τ_s term has a real and an imaginary component and is approximated as the root of Ricatti's differential equation $d\delta/d\tau_s - 2\delta^2\tau_s + 1 = 0$. A detailed explanation of how τ_s is determined is given in Ref. 22.

$k_2 = \frac{\omega}{c_o}\left\{\epsilon_2 + \frac{i\sigma\mu_o c_o^2}{\omega}\right\}^{1/2}$ = wave number of the earth.

$$\delta = \frac{i\left(\frac{k_2}{k_1}\right)^2}{(k_1 a_e)^{1/3}\left[\left(\frac{k_2}{k_1}\right)^2 - 1\right]^{1/2}}$$

ϵ_2 = permittivity of the earth. The relative permittivity ϵ_2/ϵ_o is about 15 for land, and 80 for sea.

σ = conductivity of the earth (mho/meter). ϵ_2 and σ vary as functions of weather, soil conditions, etc. Conductivity is a measure of the electrical "absorbancy" of a medium.

μ_o = permeability of free space = 1.26×10^{-6} henry/meter.

REFERENCES

(1) J. R. Johler, W. J. Kellar, and L. C. Walters. Phase of the low radiofrequency ground wave. National Bureau of Standards Circular 573, 1956.

(2) C. L. Worrell. Production of LORAN-C reliability diagrams: Computation of the maximum usable groundwave signal limit. In preparation.

(3) S. N. Samaddar. Weather effects on LORAN-C propagation. Navigation 27(1):39-53, 1980.

U.S. Coast Guard. Specification of the LORAN-C transmitted signal. Draft report, 17 August, 1979.
(4) Page 21.
(5) Enclosure (2), pages 1-3.

(6) International Radio Consultative Committee (CCIR). Report 322: World distribution and characteristics of atmospheric radio noise. International Telecommunication Union, Geneva, 1964.

(7) Arthur D. Watt. VLF Radio Engineering, page 183. Pergamon Press, 1967.

(8) International Telephone and Telegraph Corp. Reference Data for Radio Engineers, page 28-7. Howard W. Sams and Company, Inc., New York, Fifth Edition, October 1968.

(9) R. R. Gupta. Loran-C secondary phase and skywave study: groundwave prediction techniques. The Analytical Sciences Corporation, Technical Information Memorandum 735-3, 30 July, 1976.

(10) S. N. Samaddar. The theory of Loran-C ground wave propagation - A review. Navigation 26(3):173-187, 1979.

(11) P. David and J. Voge. Propagation of Waves, pages 83-88. Translated by J. B. Arthur. Pergamon Press, 1969.

(12) G. Millington. Ground wave propagation over an inhomogeneous smooth earth. Proceedings of the Institute of Electrical Engineers, part 3, 1949. Cited in Refs. 9-11.

(13) Jansky and Bailey Division of Atlantic Research Corportation. The LORAN-C system of navigation. Washington, D.C., February 1962.

(14) Ed Bregstone, U.S. Coast Guard. Private communication, October, 1980.

(15) G. H. Trow and A. H. Jessell.
The presentation of the fixing accuracy of navigation systems.
The Journal of Navigation 1:313-337, 1948.

(16) B. W. Sitterly.
Demonstrations concerning the geometry of LORAN lines.
In J. A. Pierce, A. A. McKenzie, and R. H. Woodward, editors, LORAN, M.I.T. Radiation Laboratory Series, Appendix C, McGraw-Hill, 1948.

(17) T. Hiraiwa.
On the 95 percent probability circle of a vessel's position.
The Journal of Navigation 20(3):258-270, 1967.

(18) T. Hiraiwa.
On the 95 percent probability circle of a vessel's position-II.
The Journal of Navigation 33(2):223-226, 1980.

(19) H. Bremmer.
Terrestrial Radio Waves.
Elsevier Publishing Company, Inc., 1949.

(20) James R. Wait.
Electromagnetic Waves in Stratified Media.
The Macmillan Company, 1962.

(21) Jansky and Biley Division of Atlantic Research Corporation.
Propagation data for interference analysis, volume 1, chapter VII.
Washington, D.C., January 1962.

(22) J. R. Johler, L. C. Walters, and C. M. Lilley.
Low- and very low- radiofrequency tables of ground wave parameters for the spherical earth theory: The roots of Riccati's differential equation (supplementary numerical data for NBS circular 573).
National Bureau of Standards Technical Note number 7, no publication date given.

(23) International Telephone and Telegraph Corp.
Reference Data for Radio Engineers, page 26-2.
Howard W. Sams and Company, Inc., New York, Fifth Edition, October, 1968.

(24) U. S. Coast Guard.
Specification of the LORAN-C transmitted signal.
Draft report, 17 August, 1979, page 15.